10^{th} **World Congress on Structural and Multidisciplinary Optimization**
May 19 - 24, 2013, Orlando, Florida, USA

Density Filter Control of Thickness-to-Length Change of Composite Structures

Dženan Hozić†, Anders Klarbring†, Bo Torstenfelt‡

† dzenan.hozic@liu.se, anders.klarbring@liu.se, Division of Mechanics, Department of Management and Engineering, Institute of Technology, Linköping University, SE-581 83 Linköping Sweden
‡ bo.torstenfelt@liu.se, Division of Solid Mechanics, Department of Management and Engineering, Institute of Technology, Linköping University, SE-581 83 Linköping Sweden

1. Abstract

The homogenized material optimization (HMO) problem is a novel structural optimization problem that we have developed for optimization of fiber reinforced composite structures. In the HMO problem we apply a smeared-out approach to model the material properties of fiber reinforced composite materials. The objective of the HMO problem is to maximize the stiffness of a composite structure by means of finding the optimal distribution of composite material, belonging to a fixed set of fiber orientations, across the design domain. In order to obtain manufacturable solutions, we have introduced a linear density filter as a restriction method to control the thickness variation across the design domain. To examine the effect of the density filter on the thickness variation and the objective function value of composite structures, obtained in the HMO problem, we have performed numerical tests for different load cases, mesh densities and range of the filter radius.

It is observed that for the present problem the thickness variation was mesh-independent. Both the thickness variation and objective function value depend on the load case used in the HMO problem. For all load cases the thickness variations exhibits an approximately piece-wise linear behaviour for increased filter radius. Furthermore, it was observed that an increase of filter radius would result in an moderate increase in objective function value for the solutions obtained from the HMO problem. From these results we conclude that by using a density filter, the HMO problem can be used to obtain manufacturable designs for composite structures.

2. Keywords: homogenized material optimization, composite structures, density filter, structural optimization.

3. Introduction

Structural optimization of composite structures is a research field that gains in interest as the use of fiber reinforced composite material increases. The manufacturing process of composite structures requires plies of fiber reinforced composite material to be stacked in a predefined order, lay-up sequence, to form the structure. Due to the material properties of the fiber reinforced composite plies, the mechanical behaviour of composite structures is dependent on the lay-up sequence of the plies. To generate a manufacturable composite structure it is important to control the thickness variation throughout the composite structure.

To further expand on the structural optimization of fiber reinforced composite structures we have developed the homogenized material optimization (HMO) problem, where we apply an smeared-out approach to model the material properties of fiber reinforced composite material. The objective of the HMO problem is to maximize the stiffness of a composite structure by means of finding the optimal distribution of composite material, belonging to a fixed set of fiber orientations, across the design domain. To take into account manufacturability of the composite structure we have introduced a linear density filter on the design variables of the HMO problem, as a restriction method to control the thickness variation across the design domain.

To the best of the authors knowledge the method described here has not previously been used for optimization of composite structures. So far most of the research has been focused on developing optimization methods that find the optimal lay-up sequences for predefined structures, e.g., Stegmann and Lund, see [1], developed the discrete material optimization (DMO) method, in which the objective is to maximize the stiffness of the composite structure by finding a lay-up sequence of plies with optimal fiber orientations and material choice, chosen from a pre-defined set of candidate composite materials and fiber orientations. To solve the DMO problem the authors have used gradient based mathematical programming techniques. Javidran and Nouri, see [2], used a simulated annealing optimization algorithm for design of laminated composites with required stiffness properties. In the problem statement the objective was to minimize the sum of squared differences between calculated and required effective stiffness properties. Design constraints were set on the ply thicknesses, fiber orientation of each ply and the total thickness of plies with a given fiber orientation. Diaconu and Sekine, see [3], use lamination parameters, see [4], to find the optimal lay-up sequence for long laminated cylindrical shells. The optimization statement was to maximize the buckling loads on the shells, while a set of lamination parameters are used as design variables.

The focus of the present paper is to examine the effect of the density filter on the thickness variation of the composite structure obtained by solving the HMO problem and by doing so, investigating if a manufacturable composite structure can be obtained using the HMO problem.

4. Homogenized Material Optimization Problem

The Homogenized Material Optimization (HMO) problem concerns optimization of composite structures. It is inspired from the sizing optimization class of structural optimization problems, see [5]. In the present version of the HMO problem we are considering composite structures that are made up of composite plies with fiber orientations belonging to the set

$$\Theta = \{0^\circ, +45^\circ, -45^\circ, 90^\circ\}.$$

Moreover, we are only considering composite structures with symmetric lay-up sequences. That is, the composite plies making up the composite structure are ordered such that there is a symmetry about the mid-plane of the composite structure.

4.1. Material Properties of Fiber Reinforced Composites

The composite structure consists of unidirectional fiber reinforced composite plies, where the fibers in each ply are ordered in the same direction, these composite plies exhibit orthotropic material properties. Elements of the material coefficient matrix $\boldsymbol{Q}$ of a composite ply are given in the problem-fixed (x_1, x_2, z) coordinate system as

$$\begin{Bmatrix} Q_{11} \\ Q_{12} \\ Q_{22} \\ Q_{16} \\ Q_{26} \\ Q_{66} \\ Q_{44} \\ Q_{45} \\ Q_{55} \end{Bmatrix} = \begin{bmatrix} c^4 & 2c^2s^2 & s^4 & 4c^2s^2 & 0 & 0 \\ c^2s^2 & c^4+s^4 & c^2s^2 & -4c^2s^2 & 0 & 0 \\ s^4 & 2c^2s^2 & c^4 & 4c^2s^2 & 0 & 0 \\ c^3s & cs^3-c^3s & -cs^3 & 2(cs^3-c^3s) & 0 & 0 \\ cs^3 & c^3s-cs^3 & -c^3s & 2(c^3s-cs^3) & 0 & 0 \\ c^2s^2 & -2c^2s^2 & c^2s^2 & c^4+s^2-2c^2s^2 & 0 & 0 \\ 0 & 0 & 0 & 0 & c^2 & s^2 \\ 0 & 0 & 0 & 0 & -cs & cs \\ 0 & 0 & 0 & 0 & s^2 & c^2 \end{bmatrix} \begin{Bmatrix} \bar{Q}_{11} \\ \bar{Q}_{12} \\ \bar{Q}_{22} \\ \bar{Q}_{66} \\ \bar{Q}_{44} \\ \bar{Q}_{55} \end{Bmatrix}. \tag{1}$$

$$c = \cos\theta \quad s = \sin\theta$$

Here $\bar{Q}_{ij}$ in Eq.(1) above represent the elements of the material coefficient matrix in the ply-fixed $(\bar{x}_1, \bar{x}_2, z)$ coordinate system. $\bar{Q}_{ij}$ is expressed in terms of engineering constants as

$$\begin{aligned} \bar{Q}_{11} &= \frac{E_1}{1-\nu_{12}\nu_{21}} \quad & \bar{Q}_{12} &= \frac{\nu_{12}E_2}{1-\nu_{12}\nu_{21}} \quad & \bar{Q}_{22} &= \frac{E_2}{1-\nu_{12}\nu_{21}} \\ \bar{Q}_{66} &= G_{12} & \bar{Q}_{44} &= G_{23} & \bar{Q}_{55} &= G_{13}, \end{aligned} \tag{2}$$

where E_1, E_2 are the Young's modulus, G_{12}, G_{23}, G_{13} are the shear modulus and ν_{12}, ν_{21} are the Poisson's ratios of a unidirectional fiber-reinforced composite ply, see [6]. The transformation from the ply-fixed $(\bar{x}_1, \bar{x}_2, z)$ to problem-fixed (x_1, x_2, z) coordinate system in Eq.(1) is given by a counter-clockwise sense rotation of fibers in the plies according to Fig. 1 below, where θ corresponds to a fiber orientations belonging to Θ.

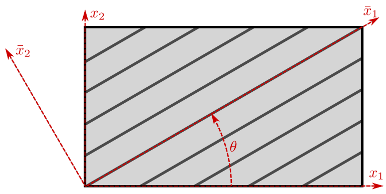

Figure 1: Transformation from $(\bar{x}_1, \bar{x}_2, z)$ to (x_1, x_2, z)-coordinate system

4.2. Finite Element Discretization

The design domain of the composite structure is divided into a number of finite element $\Omega_e, 1, \ldots, N_e$. The stiffness matrix for each element Ω_e of the design domain representing a symmetricly stacked composite structure is given by

$$\boldsymbol{k}_e = \int_{\Omega_e} \int_{-h_e/2}^{h_e/2} \left(\left(\boldsymbol{B}_e^{mem}\right)^T \boldsymbol{Q}_e \boldsymbol{B}_e^{mem} + z^2 \left(\boldsymbol{B}_e^{cur}\right)^T \boldsymbol{Q}_e \boldsymbol{B}_e^{cur} \right) dz d\Omega_e, \tag{3}$$

where $\boldsymbol{B}_e^{mem}$ and $\boldsymbol{B}_e^{cur}$ are the strain displacement matrices for membrane and curvature strains respectively, $\boldsymbol{Q}_e$ is the material coefficient matrix of element Ω_e with elements as in Eq.(1) and z is the thickness variable. Each element Ω_e contains variable amounts of composite material with fiber orientations $\theta \in \Theta$. To take into account this variation of material properties when modelling the element material coefficient matrix $\boldsymbol{Q}_e$ we apply the following linear mixing rule

$$\mathbf{Q}_e = \sum_{\theta \in \Theta} \frac{\delta_e^\theta}{h_e} \mathbf{Q}_e^\theta, \tag{4}$$

where $\boldsymbol{Q}_e^\theta$ are the material properties for a fixed fiber orientation $\theta \in \Theta$, δ_e^θ is the total amount of composite material with fiber orientation θ in element Ω_e and h_e is the total thickness of element Ω_e, which is given by

$$h_e = \sum_{\theta \in \Theta} \delta_e^\theta. \tag{5}$$

The effect of applying the mixing rule in Eq.(4) is a uniform distribution of material properties $\boldsymbol{Q}_e^\theta$ associated to each fiber orientation $\theta \in \Theta$, throughout the thickness of the element.

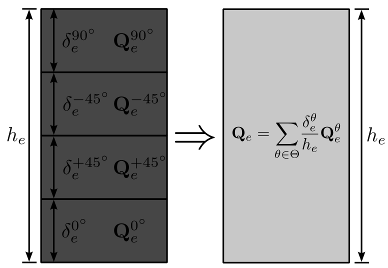

Figure 2: Distribution of material properties in an element Ω_e

By doing so the material properties of each fiber orientation $\theta \in \Theta$ are smeared-out and an homogenization of the material properties is achieved across the entire element, as illustrated in Fig. 2. The strain displacement matrices $\boldsymbol{B}_e^{mem}$, $\boldsymbol{B}_e^{cur}$ and material coefficient matrix $\boldsymbol{Q}_e^\theta$ are independent of the thickness variable z and we assume that each element has a constant thickness h_e. Then the element stiffness matrix $\boldsymbol{k}_e$ in Eq.(3), when substituting Eq.(4), becomes

$$\boldsymbol{k}_e = \sum_{\theta \in \Theta} \left(\delta_e^\theta \left(\boldsymbol{k}_e^\theta\right)^{inplane} + \delta_e^\theta h_e^2 \left(\boldsymbol{k}_e^\theta\right)^{bending} \right), \tag{6}$$

where

$$\left(\boldsymbol{k}_e^\theta\right)^{inplane} = \int_{\Omega_e} \left(\boldsymbol{B}_e^{mem}\right)^T \boldsymbol{Q}_e^\theta \boldsymbol{B}_e^{mem} d\Omega_e, \qquad \left(\boldsymbol{k}_e^\theta\right)^{bending} = \int_{\Omega_e} \frac{1}{12} \left(\boldsymbol{B}_e^{cur}\right)^T \boldsymbol{Q}_e^\theta \boldsymbol{B}_e^{cur} d\Omega_e. \tag{7}$$

The global stiffness matrix is obtained as

$$\boldsymbol{K}(\boldsymbol{\delta}) = \sum_{e=1}^{N_e} \boldsymbol{C}_e^T \boldsymbol{k}_e \boldsymbol{C}_e, \tag{8}$$

where $\boldsymbol{C}_e$ is a kinematic matrix that properly positions each $\boldsymbol{k}_e$ in the global stiffness matrix $\boldsymbol{K}(\boldsymbol{\delta})$. The global stiffness matrix is a function of the design variable vector $\boldsymbol{\delta}$ which is defined as

$$\boldsymbol{\delta} = \left(\boldsymbol{\delta}_1^T, \ldots, \boldsymbol{\delta}_e^T, \ldots, \boldsymbol{\delta}_{N_e}^T\right)^T, \qquad \boldsymbol{\delta}_e = \left(\delta_e^{0^\circ}, \delta_e^{+45^\circ}, \delta_e^{-45^\circ}, \delta_e^{90^\circ}\right)^T. \tag{9}$$

4.3. Restriction Method

To control the thickness variation of the composite structure in the HMO problem, there needs to be a coupling between design variables of adjacent elements of the design domain. This is achieved by using a basic linear density filter on the design variables, see [7],[8]. The filtering of the design variables mathematically reads

$$\delta_e^\theta\left(\boldsymbol{x}^\theta\right) = \sum_{j=1}^{N_e} W_{ej} x_j^\theta, \tag{10}$$

where $\delta_e^\theta\left(\boldsymbol{x}^\theta\right)$ are the filtered design variables that are used to calculate the stiffness and volume of the composite structure and x_e^θ are the unfiltered design variable that become the independent variables of the optimization problem, see [9]. W_{ej} in Eq.(10) is a weight matrix containing the weights of the density filter according to

$$W_{ej} = \frac{\omega_j}{\sum_{j=1}^{N_e} \omega_j}, \tag{11}$$

where the weights ω_j of the density filter are given by a cone-shaped function

$$\omega_j = \frac{R - r_j}{R}. \tag{12}$$

Here R is the radius of the cone and r_j is the distance between centroids of elements Ω_e and Ω_j. W_{ej} is zero in Eq.(10) unless the distance between the centroids of Ω_j and Ω_e is within the filter radius R. In vector form Eq.(10) reads

$$\boldsymbol{\delta}(\boldsymbol{x}) = \boldsymbol{W}\boldsymbol{x}. \tag{13}$$

4.4. Constraints in HMO

We have implemented the following constraints: The equilibrium constraint representing the response of the composite structure is given as

$$\boldsymbol{K}(\boldsymbol{W}\boldsymbol{x})\,\boldsymbol{u} = \boldsymbol{F}, \tag{14}$$

where $\boldsymbol{K}(\boldsymbol{W}\boldsymbol{x})$ is the stiffness matrix in Eq.(8) expressed as a function of the filtered design variables in Eq.(13), $\boldsymbol{u}$ is the displacement vector of the structure and $\boldsymbol{F}$ is the force vector representing the applied load case. The first of two design constraints is set on the total volume V of the composite structure according to

$$\sum_{\theta\in\Theta}\sum_{e=1}^{N_e} a_e \delta_e^\theta\left(\boldsymbol{x}^\theta\right) = \sum_{\theta\in\Theta}\sum_{e=1}^{N_e}\sum_{j=1}^{N_e} a_e W_{ej} x_j^\theta = V, \tag{15}$$

where a_e is the area of element Ω_e. The volume constraint in Eq.(15) is interpreted in the HMO problem as an upper limit on the total amount of composite material that is allowed to be used in the design domain. The second design constraint is a box constraint on each unfiltered design variable x_j^θ:

$$\underline{x_j^\theta} \leq x_j^\theta \leq \overline{x_j^\theta}, \tag{16}$$

Note, due to the properties of W_{ej} the filtered design variables $\delta_e^\theta\left(\boldsymbol{x}^\theta\right)$ in Eq.(10) as well as x_j^θ are within the limits defined by Eq.(16), which specify that the amount of composite material with a given fiber orientation $\theta \in \Theta$ must be within the limits defined by $\underline{x_j^\theta}$ and $\overline{x_j^\theta}$.

4.5. Formulation of the Optimization Problem
The homogenized material optimization problem now reads

$$(HMO)\begin{cases} \min\limits_{\boldsymbol{u},\boldsymbol{x}} \boldsymbol{F}^T\boldsymbol{u} \\ \\ s.t \quad \begin{cases} \boldsymbol{K}\left(\boldsymbol{W}\boldsymbol{x}\right)\boldsymbol{u} = \boldsymbol{F} \\ \sum\limits_{\theta\in\Theta}\sum\limits_{e=1}^{N_e}\sum\limits_{j=1}^{N_e} a_e W_{ej} x_j^\theta = V \\ \underline{x_j^\theta} \leq x_j^\theta \leq \overline{x_j^\theta} \end{cases} \end{cases}$$

where the objective function is to minimize the compliance $\boldsymbol{F}^T\boldsymbol{u}$ and therby maximizing the stiffness of the composite structure, subjected to a load case $\boldsymbol{F}$. The HMO problem will generate an optimal composite structure by finding the best distribution of composite material for each given fiber orientation $\theta \in \Theta$ across the design domain. The implementation of the HMO problem was done in the in-house FE-software TRINITAS, see [10], where we applied an optimality criteria (OC) method for its solution, see [5],[11].

5. Thickness-to-Lenght Control of Composite Structures

In order to generate a manufacturable composite structure using the HMO problem it is important to control the rate at which the thickness of the structure changes throughout the design domain. The density filter introduces a local bound on this rate: the thickness change for a fiber orientation $\theta \in \Theta$ cannot be greater then $\left(\overline{x_j^\theta} - \underline{x_j^\theta}\right)/R$.

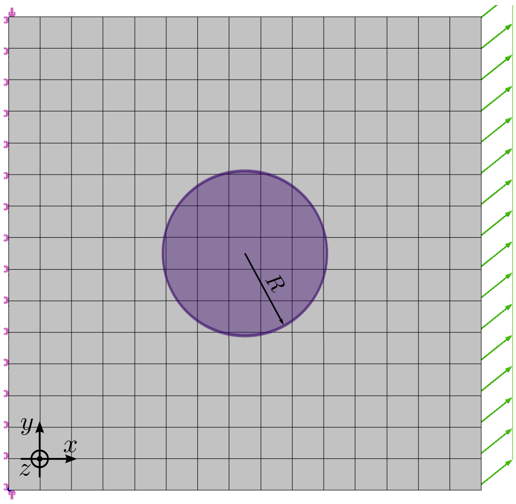

Figure 3: Discretized design domain

However, this is only an upper bound on the thickness change for material with directions $\theta \in \Theta$ and the actual influence of the filter radius R on thickness variation should be investigated by numerical tests. As a measure of thickness variation we introduce

$$\Delta = \frac{d}{h_e^{max} - h_e^{min}}, \tag{17}$$

where h_e^{max} and h_e^{min} is the maximum and minimum element thickness of the design domain, respectively, and d is the closest distance between the centers of the element with maximum thickness and the element with minimum thickness. To investigate effects of the density filter on the thickness variation in the HMO problem we have performed numerical tests for different parameter settings, i.e., filter radius R, load case $\boldsymbol{F}$ and mesh density.

6. Results

The numerical tests were done for three load cases and mesh densities, respectively. For each combination of load case and mesh density numerical tests were performed for an increasing size of the filter radius R. The parameter settings of the HMO problem for the numerical test are shown in Tab. 1. The limits

Table 1: Parameter Settings of HMO for the Numerical Tests

	N_e	$\boldsymbol{F}$	$\underline{x_j^\theta}$	$\overline{x_j^\theta}$	V	R
Load case 1	100	$1000\boldsymbol{e}_y$	0.001	4	0.1	$0 \rightarrow 2$
	625					
	1024					
Load case 2	100	$-1000\boldsymbol{e}_z$	0.001	4	0.1	$0 \rightarrow 2$
	625					
	1024					
Load case 3	100	$1000\boldsymbol{e}_y - 1000\boldsymbol{e}_z$	0.001	4	0.1	$0 \rightarrow 2$
	625					
	1024					

$\underline{x_j^\theta}$, $\overline{x_j^\theta}$ are the same for all $\theta \in \Theta$. Numerical tests preformed for parameters settings in Tab. 1 provide the results in Fig. 4.

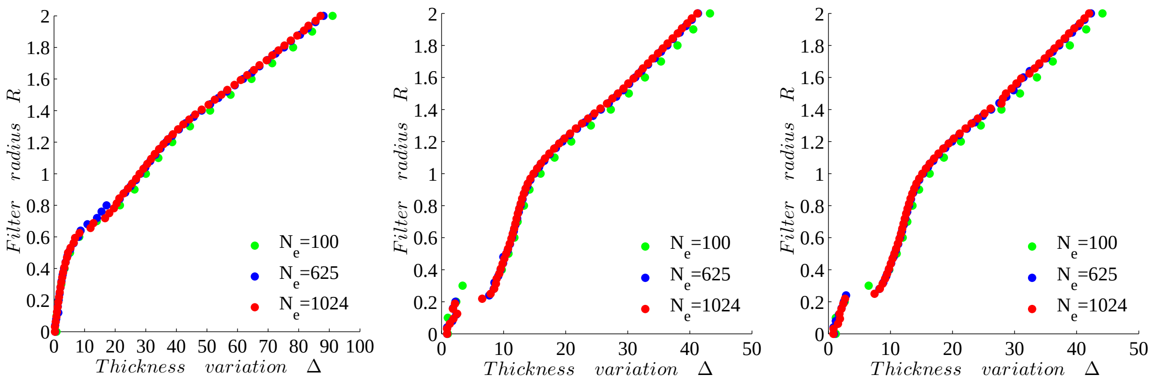

(a) Load case 1 (b) Load case 2 (c) Load case 3

Figure 4: Filter Radius R as a function of Thickness Variation Δ

In Fig. 4 plots of the filter radius R versus thickness variation Δ, for each load case in Tab. 1, are shown. For all of the load cases it is clear that thickness variation of the composite structure is not dependent on the mesh density. Further, the thickness variations in Fig. 4 all exhibit the same type of piece-wise linear continuous behaviour for increased filter radius R. However, we can observe discontinuities in thickness variations, a large one in Fig. 4b and Fig. 4 at $R \approx 0.2$ for load case 2 and 3 and also a smaller one at $R \approx 0.7$ for load case 1 in Fig. 4a. This indicates that the thickness variation depends on what type of load case is used in the HMO problem. Load case 1 and 2 are pure in-plane and out-of-plane loads, respectively, while load case 3 is a combination of the two loads. From the graphs in Fig. 4 one can conclude that if the load case contains an out-of-plane part, the behaviour of the thickness variation will correspond to Fig. 4b and Fig. 4c, while a pure in-plane load case will generate a behaviour like the one in Fig. 4a.

Table 2: Optimal Solutions of HMO for Load Case 1

	$N_e = 100$	$N_e = 625$	$N_e = 1024$
$R = 0.2$	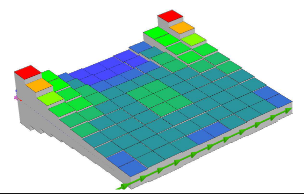	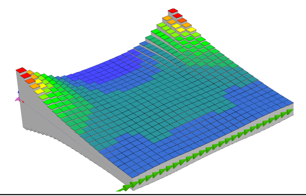	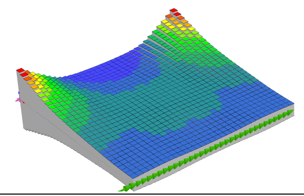
$R = 0.6$	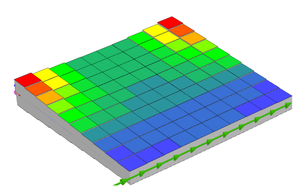	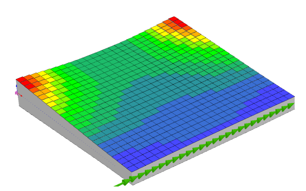	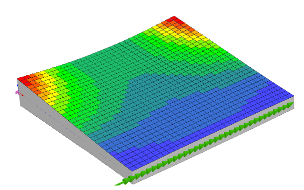
$R = 1.2$	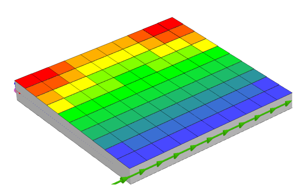	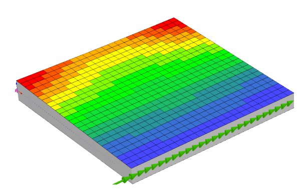	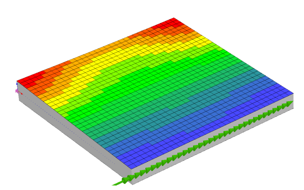

The figures in Tab. 2 show the results of the HMO problem for load case 1, which is a pure in-plane load. The solutions presented in the table show that the obtained results are mesh-independent as the solutions are only refined for increased mesh density, while the general distribution of composite material throughout the design domain remains the same. For an increase of the filter radius R the material distribution experiences changes and converges toward a linearly decaying function.

Table 3: Optimal Solutions of HMO for Load Case 2

	$N_e = 100$	$N_e = 625$	$N_e = 1024$
$R = 0.2$	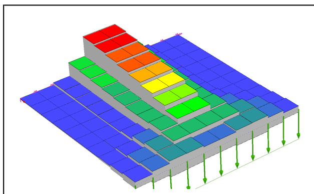	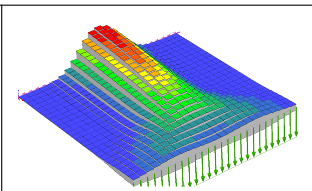	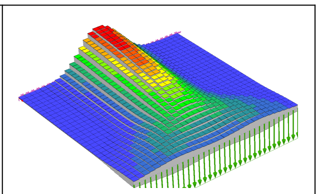
$R = 0.6$	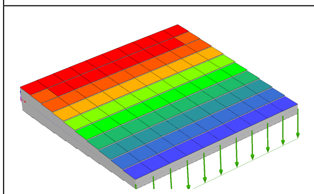	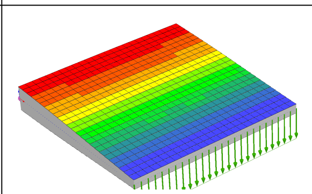	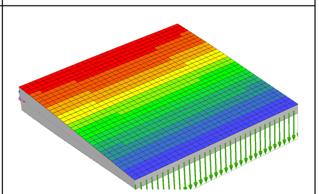
$R = 1.2$	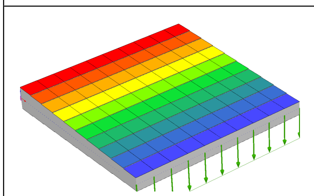	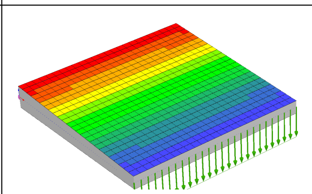	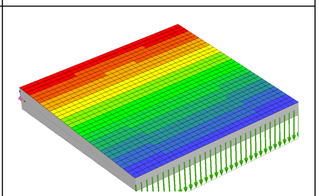

Table 4: Optimal Solutions of HMO for Load Case 3

	$N_e = 100$	$N_e = 625$	$N_e = 1024$
$R = 0.2$	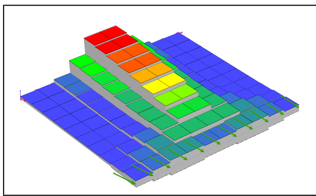	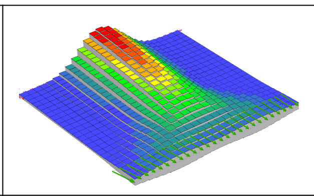	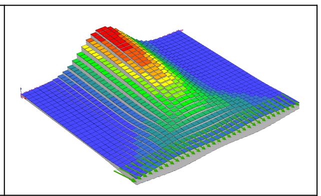
$R = 0.6$	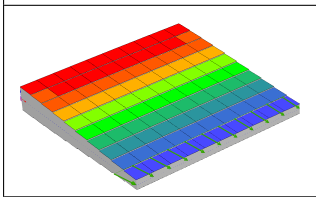	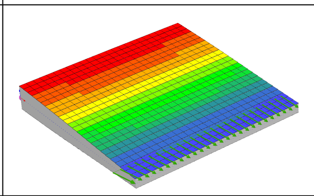	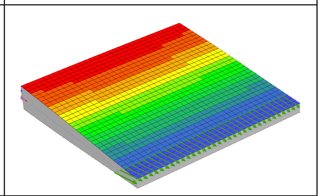
$R = 1.2$	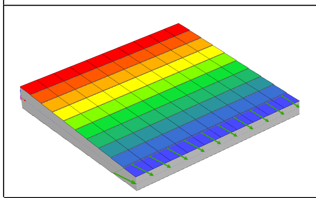	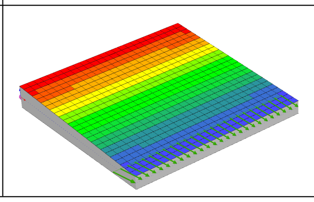	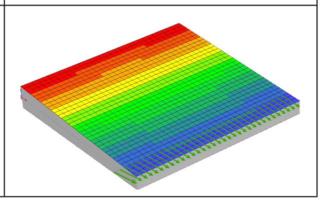

The figures in Tab. 3 and Tab. 4 represent the results of the HMO problem for load case 2 and load case 3: these load cases represent a pure out-of-plane load and a combination of in-plane and out-of-plane load, respectively. Similarly to the result of load case 1 presented in Tab. 2, the results in Tab. 3 and Tab. 4 are mesh-independent. Also they exhibit the same behaviour of converging to a linearly decaying function for increased filter radius R. However, unlike the results in Tab. 2, the results presented in Tab. 3 and Tab. 4 undergo large changes in material distribution across the design domain for small valus of filter radius R. This behaviour is also viewed in the corresponding thickness variation plots in Fig. 4b and Fig. 4c, where Δ does not increase consistently for increasing filter radius R. From a manufacturing point of view the filter radius should therefore be set to $R > 0.2$ in the present problem to generate a manufacturable feasible solution. Comparing the results in Tab. 3 and Tab. 4 we can see that the distribution of material in the design domain are very similar. This indicates that the out-of-plan part of the load dominates the solutions of the HMO problem in Tab. 4.

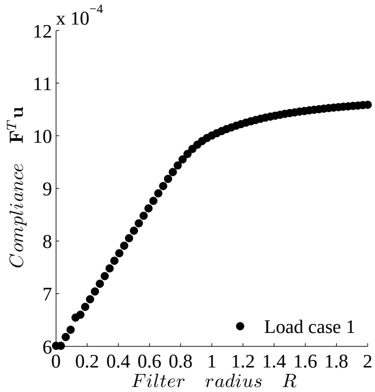

(a) Load case 1

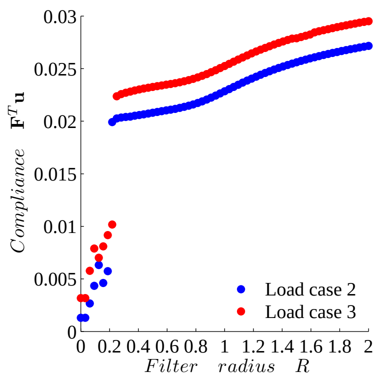

(b) Load case 2 and 3

Figure 5: Objective value plots for $N_e = 1024$

The graphs in Fig. 5 represent objective function value plots for increasing filter radius R. In Fig. 5a we see that for load case 1 the compliance approximately increases linearly for a filter radius below $R \approx 1$ Thereafter the increase in compliance is small and the compliance can be approximated as constant. Fig. 5b represent the corresponding plots for load case 2 and load case 3. In these plots we note that a sharp increase in compliance is observed at $R \approx 0.2$ for the load cases in Fig. 5b. This corresponds to a large change in the distribution of composite material as can be seen in the results presented in Tab. 3 and Tab. 4. For filter radius $R > 0.2$ in Fig. 5b we can see that the increase in the compliance in moderate.

7. Conclusions

In the present paper we have introduced the homogenized material optimization problem: a novel stiffness optimization problem for optimization of composite structures. The results of numerical test in section 6 has shown that a density filter can be effectively used in the HMO problem to control the thickness variation of composite structures. Fig. 4 together with Tab. 2, Tab. 3 and Tab. 4 show that the thickness variation of the composite structure is independent of the mesh density. Also Fig. 4 shows that the general behaviour of the thickness variation depends on what type of load case is used in the HMO problem. For the present problem it can be concluded from the results presented in Tab. 2, Tab. 3 and Tab. 4 that an filter radius of $R > 0.2$ is required to obtain an manufacturable feasible solution. In Fig. 5 we see that the objective function value is also dependent on what type of load case is applied in the HMO problem. Furthermore, it can be concluded from Fig. 5 that the filter radius R has some influence on the compliance of the composite structure, as an increases in compliance is observed for increasing filter radius R. From the results presented in the present paper it can be concluded that the HMO problem can be used to obtain manufacturable feasible solutions for composite structures.

8. Acknowlagments

We would like to thank the Swedish Foundation for Strategic Research for funding this work through the ProViking Program.

9. References

[1] J. Stegmann and E.Lund, Discrete material optimization of general composite shell structures, *International Journal for Numerical Methods in Engineering*, 62(14), 2009-2027, 2005.

[2] F. Javidrad and R. Nouri, A simulated annealing method for design of laminates with required stiffness properties, *Composite Structures*, 93(3), 1127-1135, 2011.

[3] C.G. Diaconu and H. Sekine, Layup optimization for buckling of laminated composite shells with restricted layer angles, *AIAA journal*, 42(12), 2153-2163, 2004.

[4] S.W. Tsai and H.T. Hahn, *Introduction to composite materials*, CRC Press, 1980.

[5] P.W. Christensen and A. Klarbring, *An introduction to structural optimization*, Springer Verlag, 2008.

[6] J.N. Reddy, *Mechanics of laminated composite plates and shells: theory and analysis*, CRC, 2004.

[7] T.E. Bruns and D.A. Tortorelli, Topology optimization of non-linear elastic structures and compliant mechanisms, *Computer Methods in Applied Mechanics and Engineering*, 190(26), 3443-3459, 2001.

[8] O. Sigmund, Morphology-based black and white filters for topology optimization, *Structural and Multidisciplinary Optimization*, 33(4), 401-424, 2007.

[9] A. Klarbring and B. Torstenfelt, Dynamical systems and topology optimization, *Structural and Multidisciplinary Optimization*, 42(2), 179-192, 2010.

[10] B. Torstenfelt, The TRINITAS project, *http://www.solid.iei.liu.se/Offered_services/Trinitas*, 2012.

[11] M.P. Bendsøe and O. Sigmund, *Topology optimization: theory, methods, and applications*, Springer Verlag, 2003.